Low timing jitter and intensity noise from a soliton Er-fiber laser mode-locked by a fiber taper carbon nanotube saturable absorber

Chur Kim,[1] Kwangyun Jung,[1] Khanh Kieu,[2] and Jungwon Kim[1,*]

[1]*School of Mechanical, Aerospace and Systems Engineering & KAIST Institute for Optical Science and Technology, Korea Advanced Institute of Science and Technology (KAIST), Daejeon 305-701, South Korea*
[2]*College of Optical Sciences, University of Arizona, 1630 East University Boulevard, Tucson, Arizona 85721, USA*
[*]*jungwon.kim@kaist.ac.kr*

Abstract: We characterize the timing jitter and intensity noise of an 80-MHz soliton Er-fiber laser mode-locked by a fiber taper carbon nanotube saturable absorber (ft-CNT-SA) up to the Nyquist frequency. The measured rms timing jitter is 3.0 fs (11.0 fs) integrated from 10 kHz (1 kHz) to 40 MHz offset frequency. The measured rms relative intensity noise (RIN) is 0.069% (0.021%) integrated from 10 Hz to 40 MHz (1 MHz) offset frequency. We identify that the resulting timing jitter is dominated by the Gordon-Haus jitter originated from the negative dispersion necessary for soliton mode-locking with a slow saturable absorber.

OCIS codes: (270.2500) Fluctuations, relaxations, and noise; (140.3510) Lasers, fiber; (320.7100) Ultrafast measurements; (140.4050) Mode-locked lasers; (320.7090) Ultrafast lasers.

References and links

1. T. R. Schibli, I. Hartl, D. C. Yost, M. J. Martin, A. Marcinkevičius, M. E. Fermann, and J. Ye, "Optical frequency comb with submillihertz linewidth and more than 10 W average power," Nat. Photonics **2**(6), 355–359 (2008).
2. N. R. Newbury and W. C. Swann, "Low-noise fiber-laser frequency combs," J. Opt. Soc. Am. B **24**(8), 1756–1770 (2007).
3. J. Kim, M. J. Park, M. H. Perrott, and F. X. Kärtner, "Photonic subsampling analog-to-digital conversion of microwave signals at 40-GHz with higher than 7-ENOB resolution," Opt. Express **16**(21), 16509–16515 (2008).
4. A. Khilo, S. J. Spector, M. E. Grein, A. H. Nejadmalayeri, C. W. Holzwarth, M. Y. Sander, M. S. Dahlem, M. Y. Peng, M. W. Geis, N. A. DiLello, J. U. Yoon, A. Motamedi, J. S. Orcutt, J. P. Wang, C. M. Sorace-Agaskar, M. A. Popović, J. Sun, G. R. Zhou, H. Byun, J. Chen, J. L. Hoyt, H. I. Smith, R. J. Ram, M. Perrott, T. M. Lyszczarz, E. P. Ippen, and F. X. Kärtner, "Photonic ADC: overcoming the bottleneck of electronic jitter," Opt. Express **20**(4), 4454–4469 (2012).
5. J. Kim, J. A. Cox, J. Chen, and F. X. Kärtner, "Drift-free femtosecond timing synchronization of remote optical and microwave sources," Nat. Photonics **2**(12), 733–736 (2008).
6. I. Coddington, W. C. Swann, L. Lorini, J. C. Bergquist, Y. Le Coq, C. W. Oates, Q. Quraishi, K. S. Feder, J. W. Nicholson, P. S. Westbrook, S. A. Diddams, and N. R. Newbury, "Coherent optical link over hundreds of metres and hundreds of terahertz with subfemtosecond timing jitter," Nat. Photonics **1**(5), 283–287 (2007).
7. I. Coddington, W. C. Swann, and N. R. Newbury, "Coherent multiheterodyne spectroscopy using stabilized optical frequency combs," Phys. Rev. Lett. **100**(1), 013902 (2008).
8. F. Quinlan, T. M. Fortier, M. S. Kirchner, J. A. Taylor, M. J. Thorpe, N. Lemke, A. D. Ludlow, Y. Jiang, and S. A. Diddams, "Ultralow phase noise microwave generation with an Er:fiber-based optical frequency divider," Opt. Lett. **36**(16), 3260–3262 (2011).
9. W. Zhang, Z. Xu, M. Lours, R. Boudot, Y. Kersalé, A. N. Luiten, Y. Le Coq, and G. Santarelli, "Advanced noise reduction techniques for ultra-low phase noise optical-to-microwave division with femtosecond fiber combs," IEEE Trans. Ultrason. Ferroelectr. Freq. Control **58**(5), 900–908 (2011).
10. T. K. Kim, Y. Song, K. Jung, C. Kim, H. Kim, C. H. Nam, and J. Kim, "Sub-100-as timing jitter optical pulse trains from mode-locked Er-fiber lasers," Opt. Lett. **36**(22), 4443–4445 (2011).
11. Y. Song, C. Kim, K. Jung, H. Kim, and J. Kim, "Timing jitter optimization of mode-locked Yb-fiber lasers toward the attosecond regime," Opt. Express **19**(15), 14518–14525 (2011).
12. S. Yamashita, Y. Inoue, S. Maruyama, Y. Murakami, H. Yaguchi, M. Jablonski, and S. Y. Set, "Saturable absorbers incorporating carbon nanotubes directly synthesized onto substrates and fibers and their application to mode-locked fiber lasers," Opt. Lett. **29**(14), 1581–1583 (2004).

#178904 - $15.00 USD Received 31 Oct 2012; revised 11 Dec 2012; accepted 11 Dec 2012; published 19 Dec 2012

13. Y. W. Song, S. Yamashita, C. S. Goh, and S. Y. Set, "Carbon nanotube mode lockers with enhanced nonlinearity via evanescent field interaction in D-shaped fibers," Opt. Lett. **32**(2), 148–150 (2007).
14. S. Y. Set, H. Yaguchi, Y. Tanaka, and M. Jablonski, "Ultrafast fiber pulsed lasers incorporating carbon nanotubes," IEEE J. Sel. Top. Quantum Electron. **10**(1), 137–146 (2004).
15. Y. C. Chen, N. R. Raravikar, L. S. Schadler, P. M. Ajayan, Y. P. Zhao, T. M. Lu, G. C. Wang, and X. C. Zhang, "Ultrafast optical switching properties of single-wall carbon nanotube polymer composites at 1.55 μm," Appl. Phys. Lett. **81**(6), 975–977 (2002).
16. F. Wang, A. G. Rozhin, V. Scardaci, Z. Sun, F. Hennrich, I. H. White, W. I. Milne, and A. C. Ferrari, "Wideband-tuneable, nanotube mode-locked, fibre laser," Nat. Nanotechnol. **3**(12), 738–742 (2008).
17. K. H. Fong, K. Kikuchi, C. S. Goh, S. Y. Set, R. Grange, M. Haiml, A. Schlatter, and U. Keller, "Solid-state Er:Yb:glass laser mode-locked by using single-wall carbon nanotube thin film," Opt. Lett. **32**(1), 38–40 (2007).
18. F. X. Kärtner and U. Keller, "Stabilization of solitonlike pulses with a slow saturable absorber," Opt. Lett. **20**(1), 16–18 (1995).
19. C. Ouyang, P. Shum, H. Wang, J. H. Wong, K. Wu, S. Fu, R. Li, E. J. R. Kelleher, A. I. Chernov, and E. D. Obraztsova, "Observation of timing jitter reduction induced by spectral filtering in a fiber laser mode locked with a carbon nanotube-based saturable absorber," Opt. Lett. **35**(14), 2320–2322 (2010).
20. K. Wu, P. P. Shum, S. Aditya, C. Ouyang, J. H. Wong, H. Q. Lam, and K. E. K. Lee, "Noise conversion from pump to the passively mode-locked fiber lasers at 1.5 μm," Opt. Lett. **37**(11), 1901–1903 (2012).
21. J. Kim, J. Chen, J. Cox, and F. X. Kärtner, "Attosecond-resolution timing jitter characterization of free-running mode-locked lasers," Opt. Lett. **32**(24), 3519–3521 (2007).
22. R. Paschotta, "Noise of mode-locked lasers (Part II): timing jitter and other fluctuations," Appl. Phys. B **79**(2), 163–173 (2004).
23. R. Paschotta, "Timing jitter and phase noiseof mode-locked fiber lasers," Opt. Express **18**(5), 5041–5054 (2010).
24. K. Kieu and M. Mansuripur, "Femtosecond laser pulse generation with a fiber taper embedded in carbon nanotube/polymer composite," Opt. Lett. **32**(15), 2242–2244 (2007).
25. T. K. Kim, Y. Song, K. Jung, C. H. Nam, and J. Kim, "Sub-femtosecond timing jitter optical pulse trains from mode-locked Er-fiber lasers," in *Conference on Lasers and Electro-Optics:2011—Laser Applications to Photonic Applications*, OSA Technical Digest (CD) (Optical Society of America, 2011), Paper CTuA5.
26. H. A. Haus and A. Mecozzi, "Noise of mode-locked lasers," IEEE J. Quantum Electron. **29**(3), 983–996 (1993).
27. Y. Song, K. Jung, and J. Kim, "Impact of pulse dynamics on timing jitter in mode-locked fiber lasers," Opt. Lett. **36**(10), 1761–1763 (2011).
28. L. Nugent-Glandorf, T. A. Johnson, Y. Kobayashi, and S. A. Diddams, "Impact of dispersion on amplitude and frequency noise in a Yb-fiber laser comb," Opt. Lett. **36**(9), 1578–1580 (2011).

1. Introduction

In recent years femtosecond mode-locked fiber lasers have been intensively developed and employed due to their compactness, stability, and ease of operation compared to solid-state crystal lasers. In addition, their excellent intensity, timing, phase and frequency noise characteristics have enabled mode-locked fiber laser-based applications such as low-noise frequency combs [1,2], optical sampling and photonic analog-to-digital converters [3,4], high-precision remote synchronization [5,6], precision laser spectroscopy [7], and low-noise microwave signal generation [8,9]. The optimization of noise properties in mode-locked fiber lasers will allow further advances in these high-precision applications. In particular, reduction of timing jitter enables better synchronization performance, higher optical sampling resolution, and lower microwave phase noise, to name a few. Recently sub-100-attosecond-level timing jitter has been demonstrated from stretched-pulse, nonlinear polarization evolution (NPE)-based Er- and Yb-fiber lasers by setting the intra-cavity dispersion close to zero [10,11]. This operation regime is desirable for jitter reduction because it reduces both the amplified spontaneous emission (ASE) noise-induced timing jitter and the center frequency fluctuation-induced timing jitter coupled by intra-cavity dispersion (which is also called the Gordon-Haus timing jitter) [11].

Although the standard NPE-based fiber lasers can achieve extremely low timing jitter below 1 fs, the long-term continuous operation of such lasers is often limited by the birefringence drift and polarization state sensitivity in the laser oscillator. In order to build self-starting, robust, and continuous-operating mode-locked fiber lasers, it is highly desirable to employ *real* saturable absorber devices in the laser, such as semiconductor saturable absorber mirrors (SESAMs), carbon nanotubes (CNTs) or graphene. In particular, CNT-based saturable absorbers have been extensively studied and actively used in mode-locked fiber lasers in recent years [12–14]. It has been shown that CNT-based saturable absorbers

#178904 - $15.00 USD Received 31 Oct 2012; revised 11 Dec 2012; accepted 11 Dec 2012; published 19 Dec 2012

can have short recovery time in the sub-ps-level, wide and controllable operation bandwidth, and high damage threshold [15–17]. These properties are favorable for achieving lower timing jitter in fiber lasers because shorter recovery time enables less Gordon-Haus jitter (by reducing the necessary negative dispersion magnitude [18]); wider bandwidth enables shorter pulsewidth; higher damage threshold enables higher pulse energy in the laser cavity. Although the timing jitter of CNT-mode-locked fiber lasers was previously measured by direct photodetection and a signal source analyzer [19,20], the measurement resolution over 3 MHz integration bandwidth was limited to ~30 fs due to the excess noise in the photodetection as well as the dynamic range of the signal source analyzer. Thus, the real timing jitter performance of such CNT-mode-locked fiber lasers has not yet been accurately characterized.

In this paper, we characterize the timing jitter spectral density of an 80-MHz repetition rate soliton Er-fiber laser mode-locked by a fiber taper CNT saturable absorber (ft-CNT-SA) up to the Nyquist frequency (40 MHz) using a 220-as-resolution balanced optical cross-correlator (BOC) [21]. The measured rms timing jitter integrated from 10 kHz (1 kHz) to 40 MHz offset frequency is 3.0 fs (11.0 fs). We further identified the impact of the slow saturable absorber (ft-CNT-SA in this work) on the timing jitter: the resulting jitter is dominated by the Gordon-Haus jitter originated from the negative dispersion necessary for soliton mode-locking by a slow saturable absorber, not by other possible slow saturable absorber-induced effects such as intensity noise coupling through a slow saturable absorber [22,23]. We also measured the relative intensity noise (RIN) of the ft-CNT-SA-mode-locked fiber laser, which shows excellent rms RIN of 0.069% (0.021%) integrated from 10 Hz to 40 MHz (1 MHz) offset frequency. Also note that the ft-CNT-SA is a distributed absorption device, and the laser noise performance with a distributed real SA has not been investigated thoroughly up to date. It was not clear whether this form of SA would provide better or worse noise performance compared to the other traditional types of SA (such as SESAM or NPE). The result of our work shows for the first time that the timing jitter and RIN of a fiber laser mode-locked by a distributed SA can be excellent.

2. Experimental setup

A schematic diagram of the experimental setup is shown in Fig. 1. The measurement setup is based on a similar principle as our previous work shown in [10]. Based on a similar design as shown in [24], the laser under test (LUT), an 80.3-MHz soliton Er-fiber laser mode-locked by an evanescent-field ft-CNT-SA, was manufactured by K-Photonics LLC with a compact case size of 10 cm × 14 cm × 3 cm. The total absorption of the ft-CNT-SA is ~70% distributed over ~30 mm fiber taper length. The net intra-cavity dispersion is set to –0.055 ps^2 at 1560 nm for stable soliton mode-locking, which is also experimentally confirmed by the Kelly sideband locations in the measured optical spectrum (shown in the inset of Fig. 2). The measured full width half maximum (FWHM) optical bandwidth is 8.4 nm, which corresponds to 304 fs transform-limited pulsewidth. The output power from the 50% output coupler is 5.4 mW. To obtain enough optical pulse energy for attosecond-resolution optical cross-correlation, the output power is amplified to 80 mW (1 nJ pulse energy) by an extra-cavity Er-doped fiber amplifier (EDFA). In order to accurately evaluate the timing jitter of the LUT (ft-CNT-SA-mode-locked soliton Er-fiber laser in this work), a reference laser with timing jitter equal to or lower than that of the LUT is required. For this we built an 80.3-MHz NPE-based stretched-pulse Er-fiber laser with 0.8 fs timing jitter (when integrated from 10 kHz to 40 MHz offset frequency), which has a σ-cavity structure with a piezo-electric transducer (PZT)-mounted mirror for the repetition rate locking [25]. Table 1 summarizes major laser parameters for the LUT (ft-CNT-SA-based fiber laser) and the reference laser (NPE-based fiber laser).

#178904 - $15.00 USD Received 31 Oct 2012; revised 11 Dec 2012; accepted 11 Dec 2012; published 19 Dec 2012

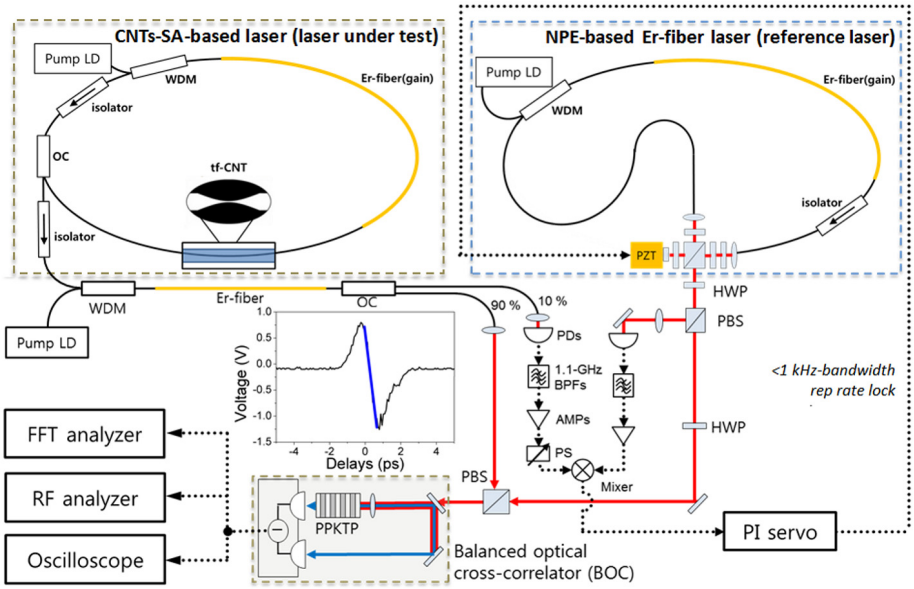

Fig. 1. Experimental setup for the BOC-based timing jitter measurement of soliton Er-fiber laser mode-locked by a CNT-SA. WDM, 980/1550 wavelength-division multiplexing coupler; OC, output coupler; PD, photodetector; BPF, 1.1-GHz bandpass filter; AMP, microwave amplifier; PS, microwave phase shifter; PBS, polarization beam splitter; HWP, half-wave plate. Solid and dotted lines indicate the optical and electrical paths, respectively. The inset shows the measured cross-correlation trace of two lasers when locking control is not applied.

Table 1. Summary of Major Laser Parameters of the LUT (ft-CNT-SA-based Fiber Laser) and the Reference Laser (NPE-based Fiber Laser)

	LUT	Reference laser
Output power (mW)	5.4	50
FWHM spectral bandwidth (nm)	8.4	68
Measured FWHM pulse duration at the BOC position (fs)	~400 (after the extra-cavity EDFA)	75
Intracavity dispersion (ps^2)	–0.055	+ 0.004
Repetition rate (MHz)	80.3	80.3
Cavity structure	Ring cavity	Sigma cavity with PZT

The amplified output from the LUT and the output from the reference laser are combined by a polarization beam splitter (PBS) and applied to a PPKTP-based BOC [21] for jitter measurement. The inset in Fig. 1 shows the output from the BOC when the repetition rates of two lasers are not locked. In order to measure the timing jitter of LUT in the linear detection range of the BOC output (the blue line indicated in the inset of Fig. 1), repetition rates of two lasers are locked by electronic locking technique [10] using the photodetected microwave signals (the 14th harmonic (1.1 GHz) of the repetition rate) generated by ~10% tapped outputs from the two lasers. In order to measure the timing jitter over wider offset frequency range, it is desirable to lower the locking bandwidth as much as possible because the timing jitter of free-running lasers can be measured only outside the locking bandwidth. On the other hand, if the locking bandwidth is too low, the total peak-to-peak integrated jitter between the two lasers can be larger than the linear detection range of the BOC (~1 ps in this work), which hinders the accurate jitter measurement. As will be also discussed in Section 3, we found that the electronic locking bandwidth of ~200 Hz allows a faithful BOC-based timing jitter spectrum measurement down to ~1 kHz offset frequency.

The output from the BOC is the sum of the timing jitter from two lasers assuming they are independent and uncorrelated. Thus the measured BOC result represents the upper limit

#178904 - $15.00 USD Received 31 Oct 2012; revised 11 Dec 2012; accepted 11 Dec 2012; published 19 Dec 2012

of timing jitter of the laser with worse performance. As will be shown in Section 3, the measured jitter from the BOC is about 4 times larger than the known jitter of the reference laser, which indicates that the measured timing jitter is mostly contributed by the LUT. For measuring the jitter spectral density, a fast Fourier transform (FFT) analyzer and a radio-frequency (RF) analyzer are used for 1 Hz – 100 kHz and 100 kHz – 40 MHz offset frequency ranges, respectively.

3. Measurement results and discussion

Curve (a) in Fig. 2 shows the measured timing jitter spectral density from the BOC output. It is ~10 dB higher than the jitter spectrum obtained for the reference laser shown in [25], which indicates that curve (a) represents the timing jitter of the LUT, i.e., the ft-CNT-SA-mode-locked Er-fiber laser. The actual timing jitter spectrum of LUT starts from ~1 kHz offset frequency because the jitter spectrum around the repetition rate locking bandwidth of ~200 Hz is distorted by the resonant peak caused by the electronic control loop. The timing jitter spectrum follows $1/f^2$ slope at low offset frequency ranging from 1 kHz to 300 kHz and $1/f^4$ slope at high offset frequency ranging from 600 kHz to 3MHz. Between 300 kHz and 600 kHz, it shows a slope transition region from $1/f^2$ to $1/f^4$. The flat noise floor above 3 MHz is caused by the shot noise in the photodetection process in the BOC. The equivalent shot noise-limited measurement resolution is 220 as for 40 MHz integration bandwidth. The rms timing jitter of the ft-CNT-SA-mode-locked Er-fiber laser is 3.0 fs (11.0 fs) when integrated from 10 kHz (1 kHz) to 40 MHz offset frequency.

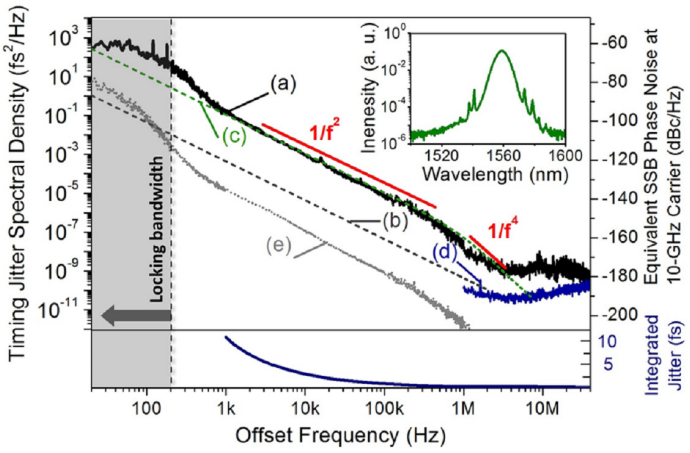

Fig. 2. (a) The measured timing jitter spectral density of CNT-SA-mode-locked Er-fiber laser. The rms timing jitter is 3.0 fs (11.0 fs) when integrated from 10 kHz (1 kHz) to 40 MHz offset frequency. (b) Predicted quantum-limited timing jitter directly originated from the ASE noise. (c) Predicted timing jitter originated from center frequency fluctuation coupled by dispersion when assuming the excess noise factor of three. (d) Predicted RIN-coupled timing jitter by the Kramers-Krönig relation. (e) Predicted RIN-coupled timing jitter by the CNT-SA. Inset: Optical spectrum of the CNT-SA-mode-locked Er-fiber laser.

In order to identify the physical mechanisms for the measured timing jitter, we used laser noise analytic models [22,23,26] and the measured and known laser parameters. Major parameters that we used in the analysis are following: total cavity loss $l_{tot} = 0.8$, intensity gain $g = 1.6$, gain bandwidth $\Delta\nu_g = 7 \times 10^{12}$ Hz, pulse bandwidth $\Delta\nu_p = 1 \times 10^{12}$ Hz, and pulse energy $E_p = 0.14$ nJ. Curve (b) shows the calculated quantum-limited timing jitter directly originated from the ASE noise, which is ~20 dB lower than the measured result. When we add the theoretical timing jitter originated from the ASE-noise-induced center frequency fluctuation coupled via intra-cavity dispersion (the Gordon-Haus jitter) assuming the excess noise factor of three, the measured data (curve (a)) fits fairly well with the analytic model

#178904 - $15.00 USD Received 31 Oct 2012; revised 11 Dec 2012; accepted 11 Dec 2012; published 19 Dec 2012

(curve (c)) based on equations in [23]. Note that excess noise factor of three is chosen here to best fit the analytic model jitter level (in the 1 kHz – 100 kHz offset frequency region) with that of the measurement. The measured jitter spectrum result is also consistent with the previous timing jitter measurement of soliton and self-similar NPE Yb-fiber lasers, where the timing jitter spectra are limited by the Gordon-Haus jitter as well [27]. Below the shot noise limited measurement floor at ~10^{-9} fs^2/Hz for >3 MHz offset frequency, the jitter spectrum will eventually reach the intensity noise-coupled jitter originated from the Kramers-Krönig relation (curve (d)).

We examined the influence of other possible slow saturable absorber-induced timing jitter effects such as intensity noise coupling by a slow saturable absorber. It is known that a slow saturable absorber with a recovery time longer than the pulse duration can translate intensity noise into timing noise [22]. In order to evaluate the impact of the intensity noise coupling via the ft-CNT-SA, we measured important characteristics of the ft-CNT-SA sample which is similar to the one used in the LUT, such as modulation depth (6%), loss (77%) and saturation fluence (150 μJ/cm^2). By using the measured RIN spectrum (curve (i) in Fig. 3) and the measured ft-CNT-SA parameters, the estimated timing jitter spectrum originated from intensity noise coupled by the ft-CNT-SA is obtained (curve (e) in Fig. 2), which is far lower than the measured jitter (curve (a)). Therefore we can conclude that the resulting jitter of the tested ft-CNT-SA-mode-locked fiber lasers is dominated by the Gordon-Haus jitter originated from the negative dispersion necessary for soliton mode-locking, not by other possible slow saturable absorber effects such as intensity noise coupling via the ft-CNT-SA. Note that the absolute accuracy of modeled spectra (curves (b)-(e) in Fig. 2) is inevitably limited because not all laser parameters can be exactly measured inside the all-fiber laser cavity (excess noise factor, for example) and we had to make some reasonable assumptions when setting the parameters. Despite some limitations, as shown above, comparison to the analytic models still provides useful insight to the observed noise properties.

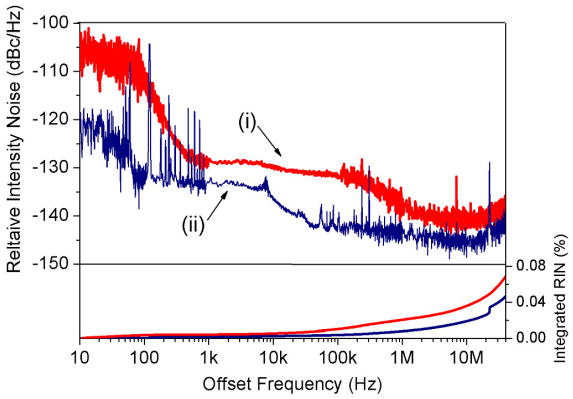

Fig. 3. Measured relative intensity noise (RIN) spectra of the CNT-SA-mode-locked fiber laser (curve (i)) and the NPE-based stretched-pulse reference laser (curve (ii)). The integration bandwidth is from 10 Hz to 40 MHz (Nyquist frequency).

We also characterize the RIN of the ft-CNT-SA-mode-locked soliton fiber laser (shown by curve (i) in Fig. 3). It shows excellent rms RIN of 0.069% (0.021%) integrated from 10 Hz to 40 MHz (1 MHz) offset frequency. For comparison, the RIN of the NPE-based reference laser is also shown by curve (ii), which has 0.047% (0.008%) integrated rms RIN from 10 Hz to 40 MHz (1 MHz). Note that the RIN of the CNT-SA-mode-locked fiber laser is already comparable (within 10 dB) to that of the stretched-pulse NPE fiber laser near zero dispersion, which is generally known to have the lowest intensity noise operation condition [11,28].

#178904 - $15.00 USD Received 31 Oct 2012; revised 11 Dec 2012; accepted 11 Dec 2012; published 19 Dec 2012

4. Conclusion

In this paper, we presented the first attosecond-resolution timing jitter characterization of an ft-CNT-SA-mode-locked soliton fiber laser. The measured rms timing jitter is 3.0 fs (11.0 fs) integrated from 10 kHz (1 kHz) to 40 MHz offset frequency. We also measured the RIN of the laser, which shows excellent rms RIN of 0.069% (0.021%) integrated from 10 Hz to 40 MHz (1 MHz) offset frequency. Note that, although the laser under test is a standard soliton Er-fiber laser and further noise optimization has not yet been performed, the demonstrated 3-fs-level jitter can already satisfy some of the most stringent timing requirements such as clocking X-ray free-electron lasers (XFELs) [5]. We further identified the impact of the ft-CNT-SA on the timing jitter that the resulting jitter is simply dominated by the Gordon-Haus jitter from the negative dispersion necessary for soliton mode-locking, not by other effects such as RIN coupling through a slow saturable absorber. This result shows that, by using a standard telecommunication 980-nm diode laser as a pump source, employing *real* saturable absorber devices such as SESAM or CNT in fiber lasers may not add additional jitter by the absorbers themselves. We expect that the development and employment of CNT or graphene saturable absorbers with shorter recovery time, which in turn reduces the necessary dispersion magnitude and resulting pulsewidth, will enable long-term stable, robust, and self-starting fiber lasers with attosecond-level timing jitter suitable for various high-precision applications outside laboratory environments.

Acknowledgment

We thank Sangho Bae for technical assistance. This research was supported by the National Research Foundation (NRF) of Korea (2010-0003974 and 2012R1A2A2A01005544).

#178904 - $15.00 USD Received 31 Oct 2012; revised 11 Dec 2012; accepted 11 Dec 2012; published 19 Dec 2012